Available online at www.sciencedirect.com
ScienceDirect
Micron 38 (2007) 121–128
micron
www.elsevier.com/locate/micron

Speckle random coding for 2D super resolving fluorescent microscopic imaging

Dror Fixler [a], Javier Garcia [b], Zeev Zalevsky [a,*], Aryeh Weiss [a], Mordechai Deutsch [c]

[a] School of Engineering, Bar-Ilan University, Ramat-Gan 52900, Israel
[b] Departamento de Optica, Universitat de Valencia, c/Dr. Moliner, 50, 46100 Burjassot, Spain
[c] Department of Physics, Bar-Ilan University, Ramat-Gan 52900, Israel

Abstract

In this manuscript we present a novel super resolving approach based upon projection of a random speckle pattern onto samples observed through a microscope. The projection of the speckle pattern is created by coherent illumination of the inspected pattern through a diffuser. Due to local interference of the coherent wave front with itself, a random speckle pattern is superimposed on the sample. This speckle pattern can be scanned over the object. A super-resolved image can be extracted from a temporal sequence of images by appropriate digital processing of the image stream. The resulting resolution is significantly higher than the diffraction limitation of the microscope objective. The new super-resolution method is demonstrated by application to fluorescence of biological samples.

Keywords: Speckle pattern; Numerical aperture; Fluorescence microscope

1. Introduction

Classical super-resolution methods are used in order to extract highly resolved images from low-quality optical imaging systems. The diffraction limit of an imaging system is inversely proportional to the numerical aperture (NA) of the optics. Thus, the aim of the super resolution is to obtain image quality corresponding to high NA using low NA optics. In microscopy, the highest quality images require use of a high-numerical aperture (NA) oil immersion objective, which are very expensive. There are several approaches related to super resolution. In all super-resolution methods, a priori information of the observed scenery is used in order to improve the spatial content. The image may be temporally static (Lohmann et al., 1996; Francon, 1952; Lukosz, 1966), wavelength band limited (Kartashev, 1960), polarized (Gartner and Lohmann, 1963) or spatially limited (Grimm and Lohmann, 1966). In all cases, the a priori data (time, wavelength, polarization or different spatial dimension) are used in order to carry the additional spatial information that cannot be transmitted through the resolution limited imaging system. After proper optical coding of the information into this additional axis it is transmitted through the optical system and then decoded and displayed on the image plane. The time multiplexing approach is good for 1D super resolution and may also be adapted to 2D resolution improvements by generating more complex 2D movement of the coding grating (Zalevsky et al., 1999a, 1999b; Mendlovic et al., 1997; Zalevsky and Mendlovic, 2003). A novel and wisely implemented super resolving approach is based upon illumination of the microscopic sample through a coherently illuminated ground glass diffuser (Garcia et al., 2005). In contrast to structured illumination microscopy (Schaefer et al., 2004; Gustafsson, 2000) where periodic patterns were projected onto the inspected samples, in this paper the illumination projects a high-resolution random speckle pattern. As in Gustafsson (2000) projection is actually a multiplication between the inspected sample and the projected pattern which is done prior to the blurring (convolution) of this product with the point spread function of the imaging system. Thus, in the Fourier plane one obtains the convolution between the spatial spectrum of the sample and the spectrum of the projected pattern while the result is multiplied by the Fourier of the point spread function. The convolution between the spectrum of the sample and the spectrum of the projected pattern may

* Corresponding author. Tel.: +972 3 5317055.
E-mail address: zalevsz@eng.biu.ac.il (Z. Zalevsky).

0968-4328/$ – see front matter © 2006 Published by Elsevier Ltd.
doi:10.1016/j.micron.2006.07.008

heterodyne information into the pass band of the optical system. In addition to the projection of the random speckle pattern we move the sample relative to the speckle pattern in order to encode the high-resolution information in the *time domain*. The high-resolution spatial information can be restored through appropriate processing of a sequence of low-resolution images. The super-resolution improvement depends on the size of the generated speckles in the sample plane. Since the speckle pattern that is used to encode and decode the spatial information of the sample is projected, it is independent of the object's structure and rather is a function of the light diffusion properties of the ground glass.

The fluorescence microscope is one of the most widely used instruments for observing living cells. However, its spatial resolution is determined by the Rayleigh diffraction limit, which is on the order of the wavelength, even with a high and expensive NA lens, such as an oil immersion lens. Techniques such as apodization (Jaquinot and Roizen-Dossier, 1964) and interferometric superposition (Leiserson et al., 2000) have been used as part of super-resolution methodologies. There exist interferometric superposition techniques which allow super resolution by computation of the diffraction patterns on the focal plane. However, it requires relatively complex data processing. Other modern resolution enhancing techniques for fluorescence microscopy (Carrington et al., 1995; Klar et al., 2001) are difficult to apply on bright-field microscopy because they usually require the high contrast from fluorescent dyes. Fluorescence microscopes routinely detect single molecules if the molecules are far enough apart (Basché et al., 1997). By the same token, several molecules at arbitrary distance may be resolved if they are spectrally distinct. Therefore, resolution must not be confused neither with single-molecule sensitivity (Weiss, 1999) nor with measuring of distances between distinct fluorescent markers (Ha et al., 1996; Bornfleth et al., 1998; Hettich et al., 2002).

This paper presents a time multiplexing method which improves the ability of a light microscope to resolve identical fluorescent structures beyond the diffraction limit of the low NA objectives which were used. Section 2 presents the theory. Experimental results are presented in Section 3, and discussed in Section 4.

2. Operation principle

Let us start by briefly presenting a simple mathematical demonstration of the operation principle. We will assume 1D objects and do 1D mathematical derivation. We will do the derivation for incoherent light. We denote by $g(x)$ the intensity distribution of the input object, by $s(x)$ the intensity distribution of the projected speckles pattern and by $P(\mu)$ the optical transfer function (OTF) of the imaging system which equals to the auto correlation of the aperture with itself. For instance, low NA objective lens yields very narrow OTF, $P(\mu)$. A lens less imaging yields $P(\mu) = \delta(\mu)$, i.e. a pinhole. We will show in the mathematical analysis below that even in this extreme case of lens less imaging, the original object's resolution will be recovered.

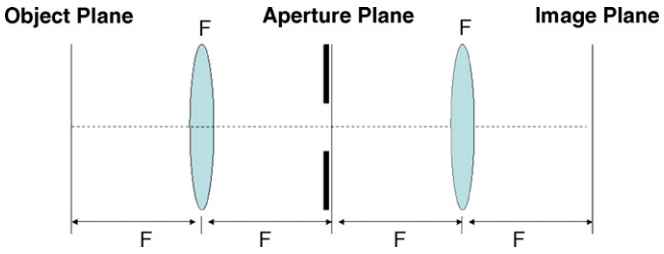

Fig. 1. Schematic sketch of a resolution limited imaging system.

The simplified imaging setup is seen in Fig. 1 and it consists of a 2-F Fourier transformer (a Fourier transformer includes a free space propagation equals to the focal length F then a lens and then additional free space propagation of F), an optical transfer function (OTF) to be denoted by P and which is placed in the Fourier plane (it equals to the auto correlation of the aperture of the lens with itself) and then additional 2-F Fourier transformer that progresses the light to the output plane. In a real microscope using infinity corrected lenses the main difference is that the second system has a longer focal length than the first, providing the nominal objective magnification. For simplicity in the calculations we keep the magnification to be unity. The derivation with magnification is straightforward. The speckles are projected on top of the object and thus we have the intensity distribution of $g(x)s(x)$. Using the basics of Fourier optics it is known that the Fourier transform of the input intensity distribution [the illuminated object $g(x)s(x)$] is multiplied by the OTF positioned at the aperture plane (Zalevsky and Mendlovic, 2003):

$$T(\mu) = P(\mu)\left[\int g(x)s(x)\exp\left(\frac{-2\pi i x\mu}{\lambda F}\right)\mathrm{d}x\right] \tag{1}$$

where λ is the wavelength and F is the focal length. We assumed that the spatial resolution of the projected speckles pattern is at least as high as that of the original object $g(x)$ that is to be recovered. Note that the convolution of the input with the random pattern, expressed in the square brackets in Eq. (1), scrambles the frequencies of the input, permitting its passage through the limited aperture represented by the OTF. This scrambling must be undone using the same random pattern for decoding, as expressed next.

Since the pattern of the speckles is shifted in time with constant velocity, one obtains:

$$T(\mu) = P(\mu)\left[\int g(x)s(x-vt)\exp\left(\frac{-2\pi i x\mu}{\lambda F}\right)\mathrm{d}x\right] \tag{2}$$

After performing additional Fourier transforming one reaches to the image plane (the output plane):

$$O(x') = \int T(\mu)\exp\left(\frac{-2\pi i x'\mu}{\lambda F}\right)\mathrm{d}\mu \tag{3}$$

The image processing decoding algorithm includes multiplying the image with identical intensity distribution of speckle pattern which is shifted in opposed direction and time averaging

the resulting distribution is:

$$O_s(x') = \int s(x' + vt)O(x')\,dt \tag{4}$$

Introducing Eqs. (2) and (3) into Eq. (4), a triple integral is obtained. The time integral can be evaluated separately as

$$\gamma(x, x') = \int s(x + vt)s(x' - vt)\,dt \tag{5}$$

which is just the autocorrelation of the speckle pattern. It can be shown that for a fully developed speckle pattern the autocorrelation can be approximated as a background value (due to the mean value of the pattern) and a much stronger additional term which is concentrated around the origin, with a typical size equals to the correlation length of the pattern (the speckle size) (Goodman, 1985). In other words, a speckle pattern is uncorrelated with the same pattern displaced more than the average speckle size. Assuming that the speckle size is small compared with the object details, we can approximate:

$$\gamma(x, x') = \kappa + \delta(x - x') \tag{6}$$

The meaning of this approximation is that the function $\gamma(x, x')$ is a spike with the resolution of the speckle pattern plus a random variation that may or may not be small depending on the number of the projected speckles.

After using the proposed approximation the output after time averaging results with:

$$O_s(x') = \int\int P(\mu)g(x) \times [\delta(x - x') + \kappa] \exp\left(\frac{-2\pi i(x - x')\mu}{\lambda F}\right) dx\,d\mu \tag{7}$$

which yields the desired result of

$$O_s(x') = g(x') \lfloor \int P(\mu)\,d\mu \rfloor + \kappa \int g(x)\,p(x' - x)\,dx \tag{8}$$

where $p(x)$ is the point spread function (PSF), obtained as the inverse Fourier transform of the OTF [$P(\mu)$]. The output has two components; the first one is, except for a multiplicative constant, a high-resolution image of the object. The second one is the convolution of the input distribution with the PSF of the system (without considering the super-resolution approach). Thus, this last term is just a low-pass version of the ideal image and must be removed in order to obtain the high-resolution image.

It is worth noticing that, even if $P(\mu)$ is a pinhole $P(\mu) = \delta(\mu)$, the first term in Eq. (8) yields $g(x')$. Since a pinhole aperture means a lens less imaging system (e.g. a pinhole camera) one may obtain a lens less microscopic imaging. All this is conditioned that the input object does not contain details smaller than the features of the random speckle pattern. Otherwise the assumption of complete non-correlated signal of Eq. (6) is not fulfilled (the correlation distance is proportional to the speckle size). From Eq. (8) one may also see that in order to recover the high-resolution image we need to subtract its low-pass version first, this will be done as part of our digital post-processing algorithm.

3. Experimental verification

3.1. Experimental preparation

In order to demonstrate the feasibility of the system we have performed laboratory experiments enhancing the resolution provided by a low-numerical aperture lens. The purpose of the experiments is to validate that a low NA lens can render a similar result, with respect to resolution, as a high-numerical aperture one. This would permit, once the proper calibration process is performed, to use low-quality lenses for routine measurements.

The process for acquiring super resolved images is as follows:

1. A high-resolution image of the speckle pattern, with no sample in place, in the plane of the sample is captured. This image constitutes the decoding speckle pattern.
2. A set of low-resolution images obtained with the low NA lens for different object displacements is acquired.
3. The reconstruction is accomplished by adding the set of images, each one multiplied by the decoding speckle pattern, undoing digitally the mechanical displacement that was made in step 2.
4. A digital post-processing (basically a high-pass filtering) will correct the transfer function that is associated with the process. The process involves the correction of the varying intensity (obtained as the average of the images) and removal of the low-pass image [see Eq. (8)]. The estimation for the

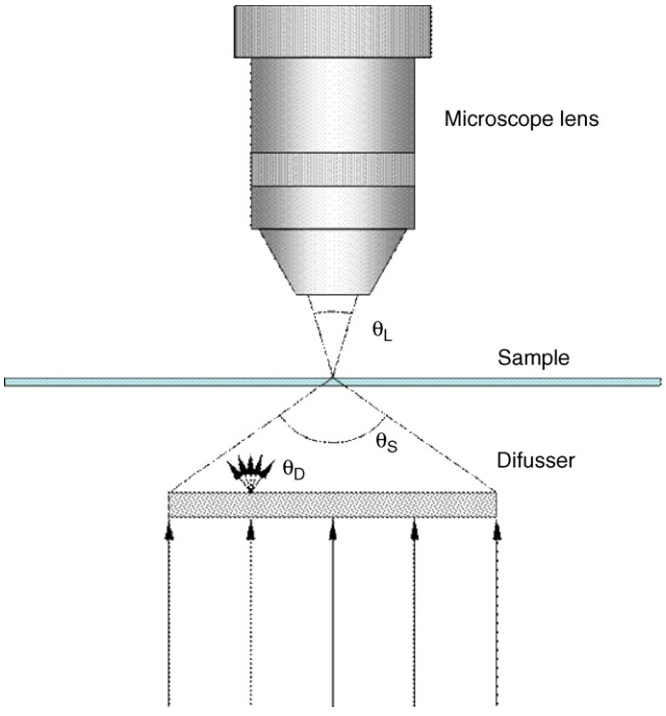

Fig. 2. System configuration.

low-pass image is made by integrating the low-resolution images in the temporal sequence without applying the decoding algorithm of step 3 (which includes the multiplication of the captured images with the speckle pattern prior to the integration in the time axis). The low-pass version of the image is subtracted from the decoded image.

The encoding speckle pattern is projected from a ground glass diffuser illuminated by means of a laser beam. The diffuser must fulfil two conditions. On one hand the diffusing angle (θ_D) must be at least that of the desired synthetic aperture. On the other hand the angular extent of the diffuser (θ_S), as seen from the sample must also be equal or larger than the desired aperture (see Fig. 2). Provided these conditions are held, the typical speckle pattern will be smaller than the desired resolution spot size.

The experiments were done on biological samples as beads and human cells that were imaged using an epi-fluorescence microscope (BX61, Olympus, Japan), with a 10 × 20 × 0.4 NA LCPlanFl objective (Olympus, Japan) and 488 nm of Ar Ion laser, Spectra-Physics (CA). Images were collected by the photometric CoolSNAP$_{HQ}$ monochrome CCD camera with a 1392 × 1040 imaging array and 6.45 × 6.45-μm pixels (Roper Scientific, Inc., Trenton, NJ). This cooled CCD camera system provides 12-bit digitization at both 10 and 20 MHz.

Human Jurkat T-lymphoblast cell line was grown in a humidified atmosphere containing 5% CO_2, in RPMI 1640 medium (Biological Industries, Israel); supplemented with 10% (v/v) heat inactivated fetal calf serum (Biological Industries, Israel), 2 mM L-glutamine, 10 mM hepes buffer solution, 1 mM sodium pyruvate, 50 U/ml penicillin, and 100 μg/ml streptomycin. The cells were washed twice with incomplete RPMI 1640 medium without phenol red, containing 10 mM HEPES buffer solution. An aliquot of 100 μl of cell suspension

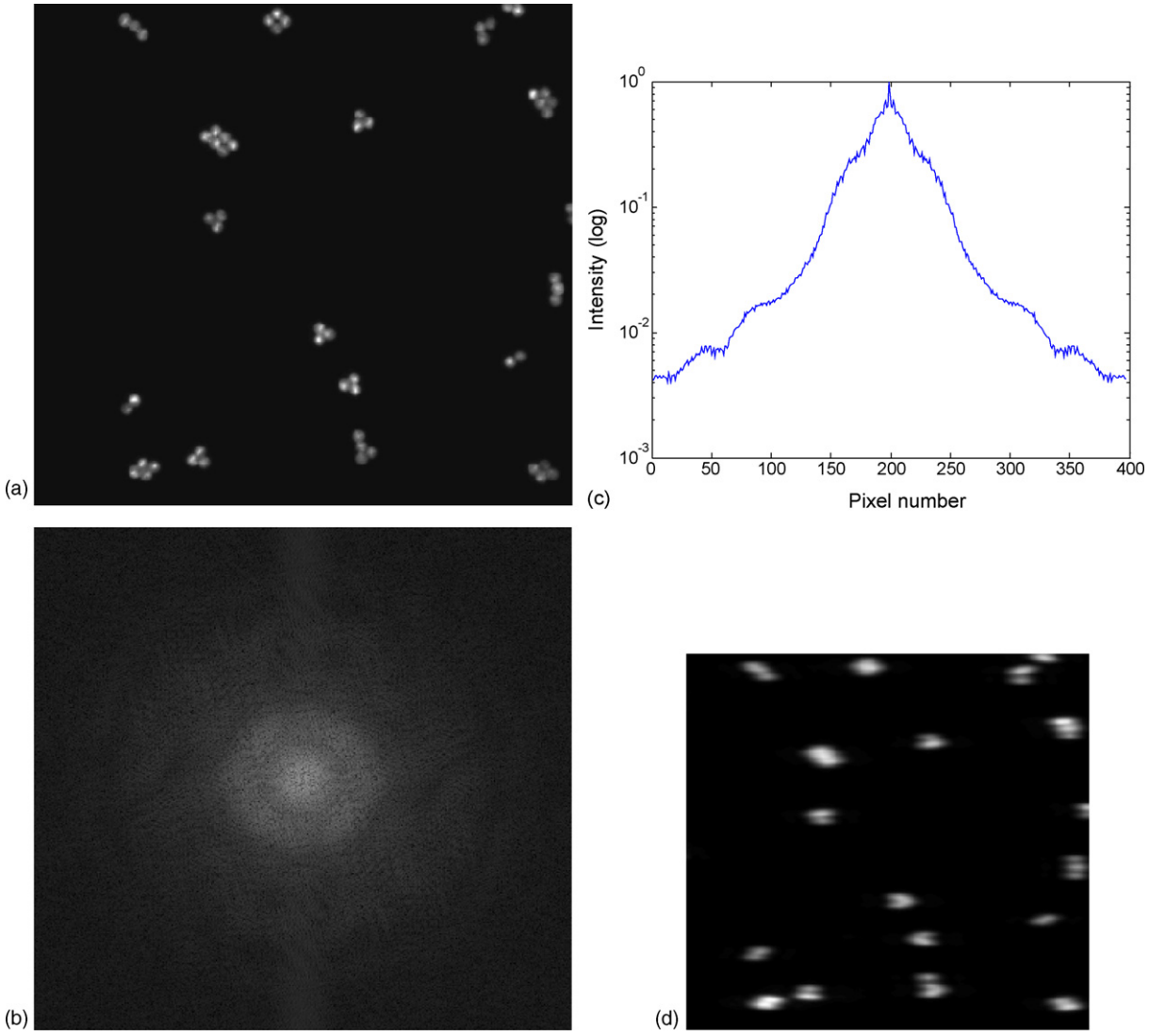

Fig. 3. One-dimensional resolution enhancement. (a) High-resolution reference image. (b) Spectrum of the high-resolution image. The intensity has been modified by a logarithmic transformation for properly displaying the low-intensity features. (c) The logarithmic plot of a profile of the spectrum. (d) Low-resolution image. (e) The spectrum of the low-pass image. (f) Logarithmic plot of a profile of the spectrum. (g) Logarithmic plot of the profile of the reconstructed spectrum. (h) The reconstructed image after subtraction of the low-pass version enhancement. (i) Spectrum of the reconstructed image. (j) Logarithmic plot of a profile of the spectrum.

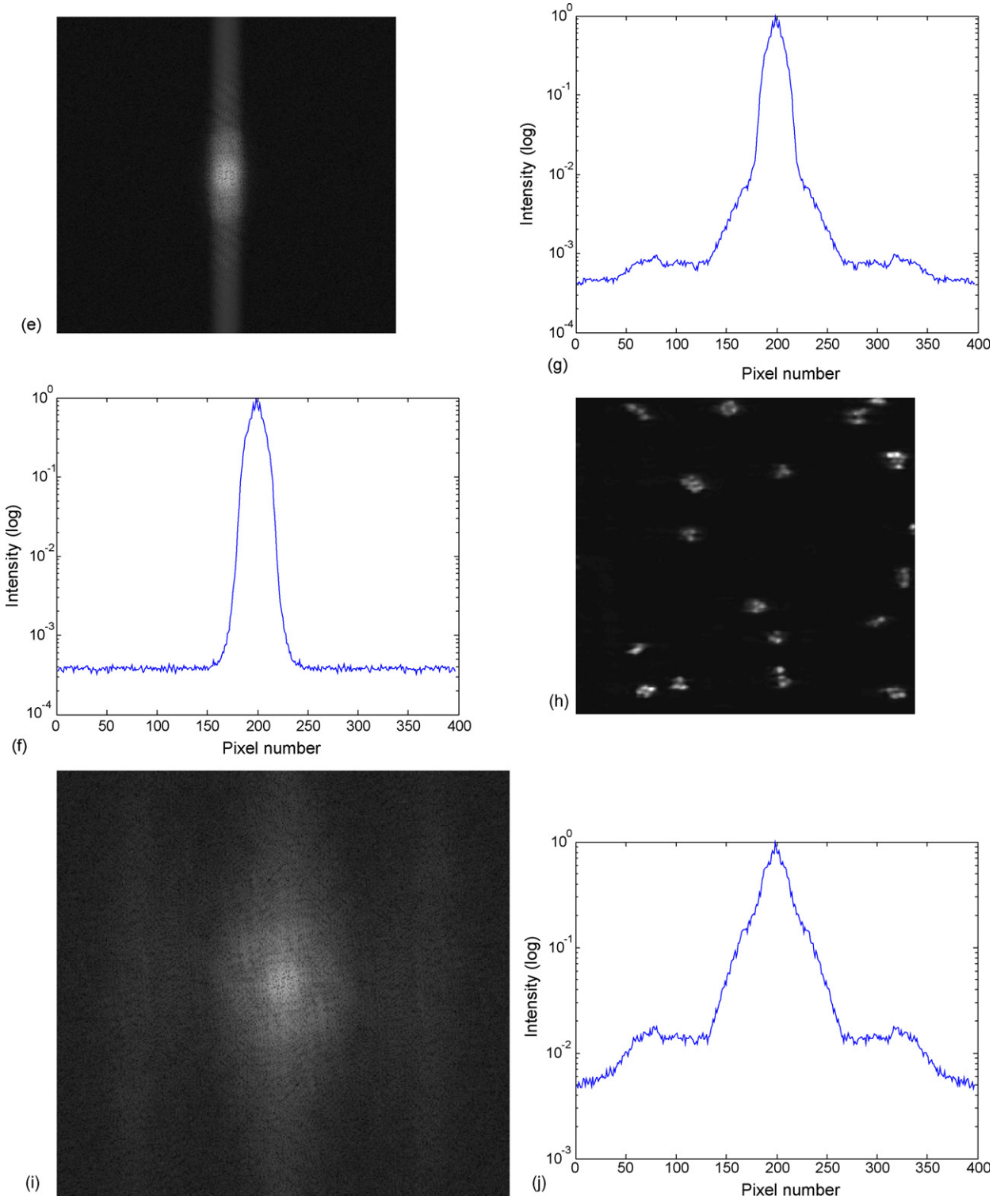

Fig. 3. (*Continued*).

(5×10^6 cells /ml) was added to 50 μl of fluorescein diacetate (FDA) staining solution (Sigma, St. Louis, MO, USA, F7378) or Tetra Metal Rhodamine (TMRM) or Rhodamine 123 (RH123) were dissolved at in PBS to a final concentration of 2 μM in PBS, and incubated at room temperature for 5 min. At the end of incubation, cells were loaded onto microscope glass and measured.

Plasma membrane integrity of FDA stained cells (Fixler et al., 1997) was checked by re-staining the same cells with propidium iodide (PI). At the end of FDA measurement, the cells were washed twice with fresh buffer and a solution containing PI (2.5 μg/ml) was added on top of the pre-tested localized cells for 5 min. Cells were then washed twice and remeasured. Positive PI cells were excluded from the analysis.

Polyscience fluorescent beads Fluoresbrite (fluorescein), 10±0.1 and 0.97 ± 0.02 μm in diameter with fluorescence intensity values of 2000–50,000 molecules of equivalent soluble fluorochromes (MESF), were used obtained from Bangs Laboratories, Inc. (IN, USA).

3.2. Microscopy experiments

In a first experiment, we have used as sample a set of the 10 μm beads. The density of beads on the sample is relatively low, giving mainly aggregates of a few beads each. A high-resolution image obtained with a 20× microscope with NA of 0.4 is shown in Fig. 3a. In Fig. 3b we present the spectrum of the high-resolution image. The intensity has been modified by a logarithmic transformation for properly displaying the low-intensity features. Note the rings due to the beads shape. In Fig. 3c we displayed the logarithmic plot of the profile of the spectrum. Note the extension of the spectrum until the image border. In Fig. 3d the image with low resolution on the *x*-axis can be observed. Obviously it is not possible to resolve some of the bead aggregates. In Fig. 3e we displayed the spectrum of the low-pass image. Note that it is limited in the horizontal axis. The ring structure is no longer visible in this direction. In Fig. 3f one may see logarithmic plot of a profile of the spectrum. Outside the central band only a uniform low-intensity random noise can be observed. The image obtained by the reconstruction process consists of the addition of a low-pass version and a high-pass version of the image. In Fig. 3g depicts the logarithmic plot of the profile of the reconstructed spectrum. Note the new information outside the central band. In Fig. 3h one may see the reconstructed image after subtraction of the low-pass version enhancement. Note that the beads are clearly resolved. The image was composed from a horizontal scan comprising 60 images. The displacement between subsequent images is of approximately three image pixels corresponding to a sample displacement (by means of the microscope stage) of 1 μm. The spectrum of Fig. 3h is presented in Fig. 3i. The ring structure is clearly visible on the image, demonstrating the existence of spatial frequencies that were not present in the low-pass version. Fig. 3j is the logarithmic plot of a profile of the spectrum. Subtraction of low-pass version enhances the high-resolution information outside the central band.

In Fig. 4 we have performed 2D super resolution with 1 μm size beads. The experimental procedure was similar to the previous experimental set of Fig. 3. In Fig. 4a we present the encoding speckle pattern projected on the fluorescent sample.

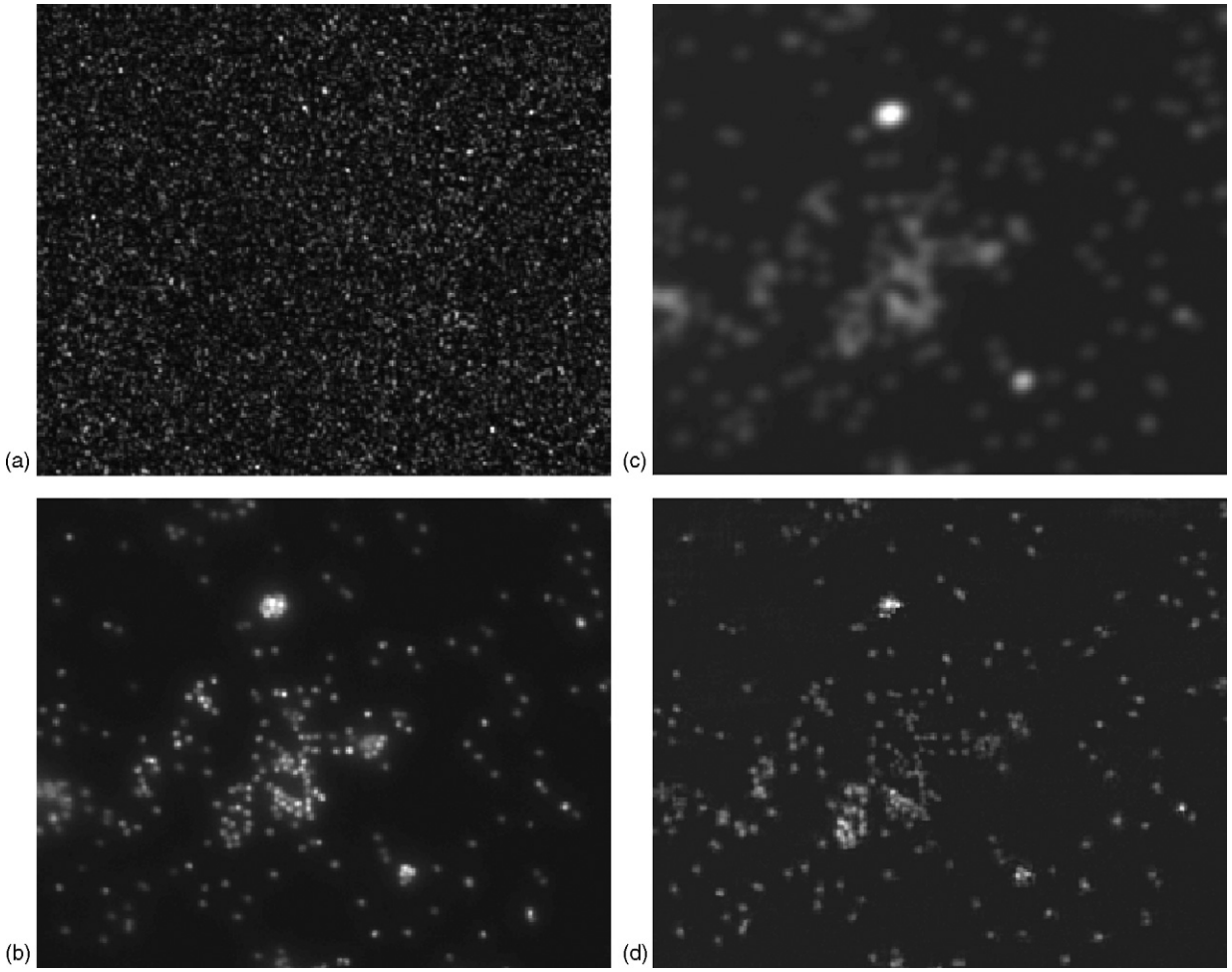

Fig. 4. Two-dimensional resolution enhancement. (a) Encoding speckle pattern. (b) High-resolution reference image. (c) Low-resolution image. (d) The reconstruction.

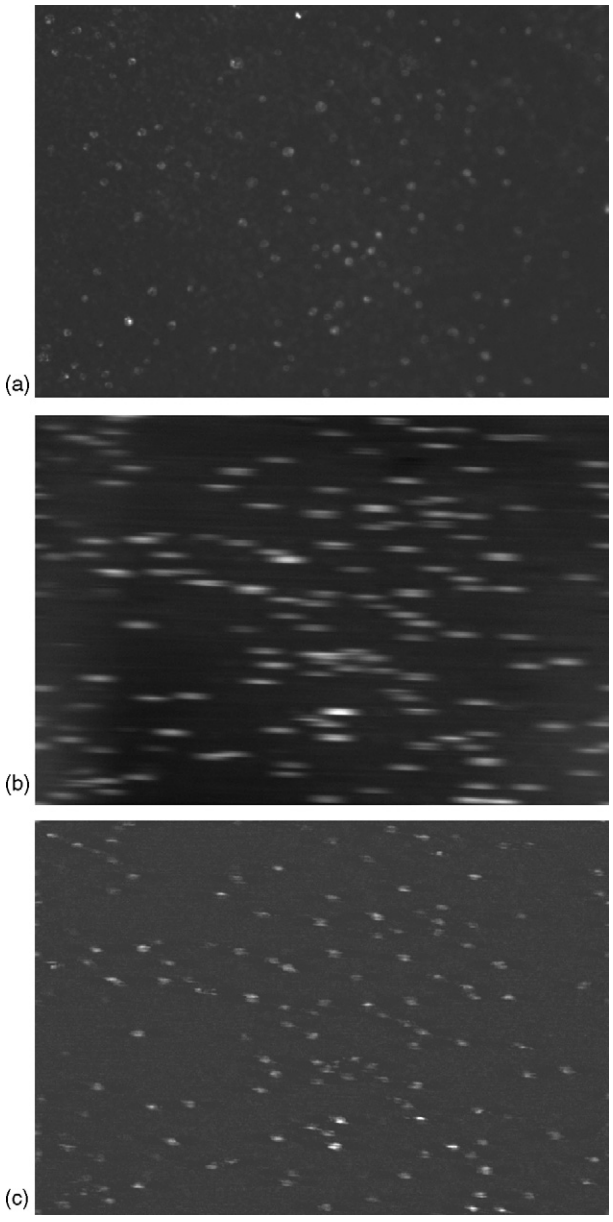

Fig. 5. Two-dimensional resolution enhancement. (a) High-resolution reference image. (b) Low-resolution image. (c) The reconstruction.

Fig. 4b shows the high-resolution reference image that we wish to obtain when low NA lens is to be in use. The low-resolution image captured with the low NA lens is seen in Fig. 4c. In Fig. 4d one may see the reconstruction we obtained which displays significant resemblance to the high-resolution reference image.

In Fig. 5 we repeated similar 2D super resolving experiment with cell samples. Once again in Fig. 5a one may see the high-resolution reference image when high NA objective lens is used. The low-resolution images captured when a low NA lens is placed are seen in Fig. 5b. Fig. 5c depicts the reconstructed image after some image processing manipulations. One may see the high resemblance between the reference image of Fig. 5a and the reconstructed image of Fig. 5c.

4. Conclusions

In this paper we have presented the usage of a new and simple super resolving approach for obtaining high-quality fluorescent imaging of biological samples through a microscope with low-quality lenses. The approach was experimentally tested in a real system and resolution improvement of more than a factor of 2 was presented. The suggested approach is practical and simple and may be useful for other various fields of microscopy for obtaining high-resolution imaging with low-numerical aperture lenses.

Acknowledgements

Javier Garcia acknowledges the support from the Spanish Ministry of Science and Education and the ministry of Science and Technology under the codes PR-2004-0543 and FIS2004-06947-C02-01.

References

Basché, T., Moerner, W.E., Orrit, M., Wild, U.P., 1997. Single-molecule Optical Detection, Imaging and Spectroscopy. VCH, Weinheim.

Bornfleth, H., Sätzler, K., Eils, R., Cremer, C., 1998. High-precision distance measurements and volume-conserving segmentation of objects near and below the resolution limit in three-dimensional confocal fluorescence microscopy. J. Microsc. 189, 118–136.

Carrington, W.A., Lynch, R.M., Moore, E.D.W., Isenberg, G., Fogarty, K.E., Fay, F.S., 1995. Super resolution three-dimensional images of fluorescence in cells. Science 268, 1483–1487.

Fixler, D., Tirosh, R., Eisenthal, A., Lalchuk, S., Marder, O., Irlin, Y., Deutsch, M., 1997. Monitoring of effector and target cell stimulation during conjugation by fluorescence polarization. Biol. Cell 89, 443–452.

Francon, M., 1952. Nuovo Cimento Suppl. 9, 283–290.

Garcia, J., Zalevsky, Z., Fixler, D., 2005. Synthetic aperture super resolution by speckle pattern projection. Opt. Exp. 13, 6073–6078.

Gartner, W., Lohmann, A.W., 1963. An experiment going beyond Abbe's limit of diffraction. Z. Physik. 174, 18.

Goodman, J., 1985. Statistical Optics. Wiley.

Grimm, M.A., Lohmann, A.W., 1966. Super resolution image for 1-D objects. JOSA A56, 1151–1156.

Gustafsson, M.G.L., 2000. Surpassing the lateral resolution limit by a factor of two using structured light illumination microscopy. J. Microsc. 198, 82–87.

Ha, T., Enderle, T., Chemla, D.S., Weiss, S., 1996. Dual-molecule spectroscopy: molecular rulers for the study of biological macromolecules. IEEE J. Select. Top. Quantum Electron. 2, 1115–1128.

Hettich, C., et al., 2002. Nanometer resolution and coherent optical dipole coupling of two individual molecules. Science 298, 385–389.

Jaquinot, P., Roizen-Dossier, B., 1964. In: Wolf, E. (Ed.), Progress in Optics, vol. III. North-Holland.

Kartashev, A.I., 1960. Optical systems with enhanced resolving power. Opt. Spectry. 9, 204–206.

Klar, T.A., Engel, E., Hell, S.W., 2001. Breaking Abbe's diffraction resolution limit in fluorescence microscopy with stimulated emission depletion beams of various shapes. Phys. Rev. E. Stat. Nonlin. Soft Matter Phys. 64 (6 Pt 2), 066613.

Leiserson, I., Lipson, S.G., Sarafits, V., 2000. Super-resolution in far-field imaging. Opt. Lett. 25, 209–211.

Lohmann, W., Dorsch, R.G., Mendlovic, D., Zalevsky, Z., Ferreira, 1996. About the space bandwidth product of optical signal and systems. JOSA A13, 470–473.

Lukosz, W., 1966. Optical systems with resolving powers exceeding the classical limit. JOSA A56, 1463–1472.

Mendlovic, D., Kiryuschev, I., Zalevsky, Z., Lohmann, A.W., Farkas, D., 1997. Two dimensional super resolution optical system for temporally restricted objects. Appl. Opt. 36, 6687–6691.

Schaefer, L.H., Shuster, D., Schaffer, 2004. Structured light illumination microscopy: artifact analysis and reduction utilizing a parameter optimization approach. J. Microsc. 216, 165–174.

Weiss, S., 1999. Fluorescence spectroscopy of single biomolecules. Science 283, 1676–1683.

Zalevsky, Z., Mendlovic, D., 2003. Optical Super Resolution. Springer-Verlag.

Zalevsky, Z., Mendlovic, D., Lohmann, A.W., 1999a. Super resolution optical systems using fixed gratings. Opt. Commun. 163, 79–85.

Zalevsky, Z., Mendlovic, D., Lohmann, A.W., 1999b. Progress in Optics, vol. XL, Ch. 4: Optical System with Improved Resolving Power.